COPY NO. 18

[redacted]

CONTRACT REQUIREMENTS	CONTRACT ITEM	MODEL	CONTRACT NO.	DATE
Exhibit E	5.1	LEM	NAS 9-1100	14 Jan 63

Type II Documentation

Primary Code No. 702

REPORT

NO. LED-510-3 DATE: 23 July 1963

"FIRE-IN-THE-HOLE" [U]

(FITH)

CODE 26512

M Solon RH
PREPARED BY:
M. Solon

CHECKED BY:
A. J. Katz

APPROVED BY:
C. W. Rathke

REVISIONS

DATE	REV. BY	REVISIONS & ADDED PAGES	REMARKS

[redacted]

INTRODUCTION

The LEM FITH problem associated with the ascent engine start-up is being investigated experimentally and analytically. This report presents the analytical and cold flow test results obtained to date, and outlines the direction for future work in this area. Earlier work including a description of the experimental setup was given in report LED 510-1, dated, 3 April 1963.

SUMMARY

(1) Downstream venting of the ascent engine exhaust gases through the annulus between the descent engine skirt and inner walls of the descent stage is very effective. Ascent nozzle flow separation was not incurred in the cold flow tests with a vent area of 1240 in^2 (full-scale). With this area, the ascent base pressure was kept to less than 1/2 the nozzle exit wall pressure. Thus the 1240 in^2 was far in excess of the venting area required to prevent nozzle flow separation. However, this configuration is no longer applicable to the LEM because the descent stage heat shield and crushing of the skirt in a lunar landing would make the downstream area unavailable.

(2) Preliminary cold flow test results for side venting through the gap between the stages with a flat plate flow deflector at the top of the descent stage indicates a minimum stage separation height of approximately 5 inches is required to keep the shock just downstream of the ascent nozzle exit. This 5 inches corresponds to approximately 1000 in^2 of venting area. Side venting between the stages without the flow deflector was found to require 16 inches stage separation height to prevent ascent nozzle separation. Besides being more effective the flow deflector keeps the exhaust gases out of the descent engine compartment and eliminates the need for ablative material on propellant feed lines, valves, etc.

(3) Present direction for the configuration is toward a flow deflector, because of the above advantages, and four porting ducts through the descent stage located downstream of the top of the descent engine. 2000 in^2 of port area is available. This is felt to be more than adequate, and could possibly be reduced, since the effectiveness of this configuration is expected to lie between that of the downstream venting and between-the-stages venting configurations.

Final choice between venting between the stages or through four ports will depend on the relative weight penalties of increased stage separation height and ducts for porting through the descent stage. Another factor may be the relative difficulty of increasing the venting area later in the program if found necessary from full-scale firings.

(4) The scaling laws used to simulate the rocket exhaust gases in the cold flow tests were investigated analytically, and were found to be applicable.

(5) Two ascent nozzles were cold flow tested; a contour and a conical. The countoured nozzle exhibited an internal oblique shock and flowed full with less venting area than that required for the conical nozzle which ran shock-free. The pressure level in the region of the ascent base was similar for both nozzles.

DISCUSSION

A. Experimental:

Cold flow testing was accomplished using nitrogen as the test fluid (γ =1.4), 7:1 area ratio ascent nozzles (contour and conical), and a 1/10 scale descent stage with constant hexagonal cross section as in the LEM proposal. Tests run with the contour nozzle include downstream venting over the descent engine and out through the annulus between the engine and stage walls (Figure 1b), and side venting between the stages without any flow deflector (Figure 1c). Conical nozzle tests included side venting between the stages both with (Figure 1f) and without a flat plate flow deflector placed on top of the descent stage.

Test results obtained with the contour nozzle were influenced by the appearance of a strong internal conical shock eminating from within the nozzle. The basic shock structure, shown schematically in Figure 1(a,b,c) was determined from Schlieren photographs, and was found to be independent of the descent stage configuration. Indications that the origin of the shock system was due to an overturning contour effect were the presence of the shock (Figure 1a) when the descent stage was removed, and a total pressure survey at the ascent nozzle exit. The resulting Mach number profile, shown in Figure 2, shows a sharp reduction in Mach number which can be attributed to the internal shock. The effect of this shock was to raise the nozzle exit static pressure at the wall, and to subsequently forestall nozzle flow separation. Hence, full nozzle flow was accomplished with less side venting area for the contour nozzle than for the shock-free conical nozzle with the same exit area ratio. Comparative side venting results for the contour and conical nozzles are shown in Figure 3. Although the level of base pressure obtained is similar, flow separation takes place with the conical nozzle because of the lower wall static pressure.

A change in the shock system was observed for the conical nozzle as noted in Figures 1d and 1e. When the flow was overexpanded ($P_e < P_b$) a conical shock system, originating from the nozzle lip, was observed. The normal shock stood considerably closer to the descent engine than in the comparable side venting configuration with the contour nozzle. A bow wave, very close to the descent engine, resulted when the base pressure was reduced.

A sharp reduction in required side venting area resulted when a flat plate was placed over the top of the descent stage. The plate acts as a flow deflector in turning the flow outward, thereby conserving a greater percentage of the momentum within the jet.

The shock structure is shown schematically in Figure 1f. A dish shaped shock was formed with the periphery of the shock remaining a constant distance upstream of the deflector plate. This distance provides a choked area at the jet periphery for the flow at a total pressure corresponding to the normal shock recovery at the mean exit Mach number. The shock stand-off distance so calculated for the cold flow model agreed within 10% of the measured value of 5 inches (full-scale). The calculated value for the full-scale engine gas properties is also approximately 5 inches. This correlation provides some confidence in the scaling procedure used to design the cold flow model.

Ascent stage base pressure data obtained from all the configurations are presented in Figure 3. The pressures were adjusted by a ratio of the chamber pressure (18 psia) predicted by the scaling laws determined analytically and the test chamber pressure (38 psia). The analytical results are discussed later, however it is noted that this data adjustment does not affect the shock structure or the vent area-nozzle separation relationship. As an example, three data points are noted at 5 inch stage separation for the side venting configuration with flow deflector. These points had test chamber pressures of 18, 24 and 38 psia, and are seen to result in approximately the same adjusted base pressure. Furthermore, the shock stand-off distance was found to be independent of the test chamber pressure.

The downstream vent configuration (1240 in^2) is seen to result in low base pressure. However, this configuration is no longer applicable to the LEM because of compartment heat shield and crushable descent engine skirt considerations. Subsequent analysis of this configuration indicated that the base pressure would be established by separation and reattachment criteria, with a base pressure level of the order of .06 psia. The higher test values obtained may be a result of test cell back pressure effects.

Venting between the stages, without using a flow deflector, required large stage separation heights. Theoretically a minimum of 16 inches would be required to prevent nozzle separation (using a more conservative conical nozzle as a criterion). The separation height was greatly reduced when the flat plate flow deflector was added. The minimum height required is approximately 5 inches for this configuration. However, the normal shock then stands right at the nozzle exit plane, and the separation height should be increased to approximately 7 inches to provide additional margin. Increasing stage separation height involves some weight penalty, and therefore the present flat plate deflector cannot be considered a final solution. This approach, however, appears to warrant further investigation to determine the feasibility of a recessed deflector which would provide the 5-7 inches required for the shock stand-off distance while reducing the required stage separation to values nearer the present 2 inch design value.

Ducting exhaust gases through four ports in the descent stage, at this time appears to offer some weight advantages over increased stage separation height. The area presently being made available is 2000 in^2. This area is felt to be more than adequate for this configuration because the effectiveness should be somewhat better than venting between the stages (1000 in^2 minimum required). Therefore, a reduction in area is expected to result from the test program.

B. Analytical:

Various FITH venting configurations were analyzed by Grumman and the Martin Marietta Corporation (GAEC P.O. 2-18833). A summary of the Martin analyses is included in the first progress report for the period 6 May through 10 July 1963. Martin's work is continuing on the analysis of a configuration with four ports located near the top of the descent engine, and is scheduled for completion at the end of July. Results of the analyses follow.

1. Configuration with four venting ports:

This configuration was analyzed at Grumman, based on a simplified flow model shown schematically in Figure 4. The objectives of the analysis were to (a) "ball park" the required port area, (b) analytically determine the effect of δ to provide correlation for the cold flow test results, and (c) determine the effect of geometric variables such as location of the descent engine and blockage presented by the engine and accessories. The primary limitations of the analysis are believed to be the assumptions of one-dimensional flow at the nozzle exit, a two-dimensional instead of axisymmetric shock system, and constant static pressure for both streams equal to the base pressure. Furthermore, the port area calculated is an effective area and does not include the effects of exit flow direction or the discharge coefficient for the four ports.

The ascent stage base pressure is shown in Figure 5 as a function of the effective port area. The lower curve is for sonic flow of both streams through the ports, and the upper curve is for constant static pressure at the ports resulting in one stream exiting at supersonic velocity. Values shown are full scale and are for the ascent engine exit conditions shown, ie., $M=4.35$, $\gamma=1.22$, $\epsilon=40{:}1$, $P_{ch}=110$ psia. Designing for a base pressure approximately equal to the nozzle exit static pressure would require approximately 1000 sq. in. of effective port area. The effective port area to prevent nozzle separation is approximately 410 sq. in., assuming the upper curve applicable.

Figure 6 shows the effect of separation distance, "A", between the descent engine and the ascent nozzle exit plane. The effect is small at low ascent base pressure, whereas at 0.4 psia a change in location from 17.4 inches to 6 inches results in approximately a 20% increase in required area.

The effect of blockage due to the engine valve package, propellant lines, etc. was taken into account by increasing the descent engine diameter, and therefore does not include the effects of asymmetry which would be present in the actual engine installation. The results, shown in Figure 7, indicate a negligable effect due to blockage at low ascent base pressure, and a 8.5% port area increase at 0.4 psia when there is 180% additional blockage.

The major effort for this analysis was spent in estimating the effect of γ, so that valid extrapolation of the cold flow test results to the rocket engine conditions might be accomplished. This consisted of varying nozzle exit Mach number and chamber pressure for γ =1.30 and 1.40, while maintaining the same geometry downstream of the ascent nozzle exit as in the LEM configuration. The combination of Mach number and chamber pressure resulting in the same ascent base pressure and port area as for the rocket engine conditions (M_e=4.35, γ =1.22, P_{ch}=110 psia) were then found. These results are shown in Figure 8, (a) for γ =1.30 and (b) for γ =1.40. The curves are bounded by two limits; the limit at the left being complete expansion in the ascent nozzle and the second limit indicates the approximate point of nozzle separation for the test conditions.

Crossplotting Figure 8b results in Figure 9, where the combination of test chamber pressure and nozzle exit Mach number for a test fluid with γ =1.4 which analytically results in the same port area and base pressure for the rocket engine conditions is shown. These results are compared to the scaling law Goethert derived for base flow modal testing. Goethert's formula essentially requires that the pressure gradient, $dp/d\Theta$, and the nozzle exit static pressure p_e, be simulated in tests where the γ of the test fluid differs from that for the rocket engine exhaust products.

The agreement between the analytical results and Goethert's formula is excellent and justifies, at least until hot flow results are obtained, the use of Goethert's scaling laws in arriving at a cold flow test configuration. Although a test Mach number and chamber pressure of 3.74 and 23 psia respectively are

indicated by Goethert's scaling parameter, the actual test Mach number corresponding to the 7:1 conical nozzle was 3.53, and most of the data was obtained at 38 psia chamber pressure. However, the lower test Mach number can be corrected by adjusting the data to the corresponding chamber pressure of 18 psia. As shown by the test results, the level of test chamber pressure does not markedly affect the flow field, and therefore adjusting the test results by the ratio of the required to the actual test chamber pressure is felt to be valid.

2. Configuration with side venting between the stages:

The Martin Co. analyzed this configuration, which included a flow deflector plate and venting area provided by stage separation. This configuration was made to look as much like the Martin-Titan II interstage compartment as possible, to provide maximum confidence in their analysis which was found to successfully correlate Titan II data.

The method uses empirically derived correlating factors, which for LEM were assumed to be the same as those derived from Titan II. The results are presented in Figure 10. The port area or stage separation height is seen to be sensitive to ascent base pressure. The adequacy of the design area is then dependent upon the accuracy in estimating the nozzle exit pressure at the wall which in turn determines the separation back pressure. Nozzle separation pressures are shown for a range of possible wall exit pressures, which at this time is an uncertainty because an ascent nozzle design has not been frozen.

3. Configuration with downstream venting:

The downstream venting configuration was analyzed by Grumman and Martin using different approaches. In Grumman's analysis the ascent base pressure was assumed to control the expansion of the exhaust gases to some Mach number distribution at the detached shock wave standing upstream of the descent engine, and hence the downstream total pressure recovery. This in turn, after considering ensuing losses and flow field due to the shocks off the descent engine skirt, would result in a required vent exit area. Or conversely, it was assumed that the exit area would establish the ascent base pressure.

Martin's analysis, on the other hand, assumed the ascent base pressure was independent of the exit area, and that it was established by the two dimensional base separation and reattachment criteria derived by Korst, etal.

The first analysis resulted in a nearly constant area (less than 1% variation) for a base pressure change of from .333 to 1.0 of the nozzle exit pressure. This indicates that the base pressure is independent of the downstream area, as long as the area is large enough to accommodate a supersonic exiting flow. The configuration analyzed was the cold flow model, and the calculated area was approximately 12% lower than for the test model.

The Martin analysis resulted in a base pressure of approximately 0.06 psia, for the full scale LEM configuration. This is considerably lower than the level obtained in the cold flow tests (0.3 psia). This discrepancy may be due, in part, to test cell pressure build-up.

FUTURE FITH WORK

Configurations incorporating a flow deflector will be emphasized in future work.

A. Experimental:

1. Cold flow tests:

1/10 scale cold flow nitrogen tests using the 7:1 area ratio conical nozzle will be continued. A LEM descent stage with provision for vent ports through the descent stage will be used. Various location and port sizes will be tested in conjunction with conical and contoured flow deflectors. Venting between the stages will be further investigated in an effort to reduce the required stage separation height.

2. Hot flow tests:

A resistance heater for use with the rig is presently being fabricated. This heater will allow hot flow testing to approximately 2300°R. Using carbon dioxide at approximately 2000°R inlet temperature would produce a γ in the range of the ascent engine exhaust products. This would allow scaling of the ascent engine nozzle as well as the descent stage, and should result in an exit Mach number and pressure profile similar to that of the full scale configuration.

The most promising porting configuration determined from the cold flow tests will be hot flow tested, and heating data, as well as gasdynamic characteristics, will be obtained.

B. Analytical:

Analysis of porting configurations will be continued by the Martin Marietta Corp. (under GAEC P.O. 2-18833 until 10 August) and by the LEM Thermodynamics Group to supplement the experimental programs.

FIGURE 1
FLOW FIELD DETERMINED FROM SCHLIEREN PICTURES

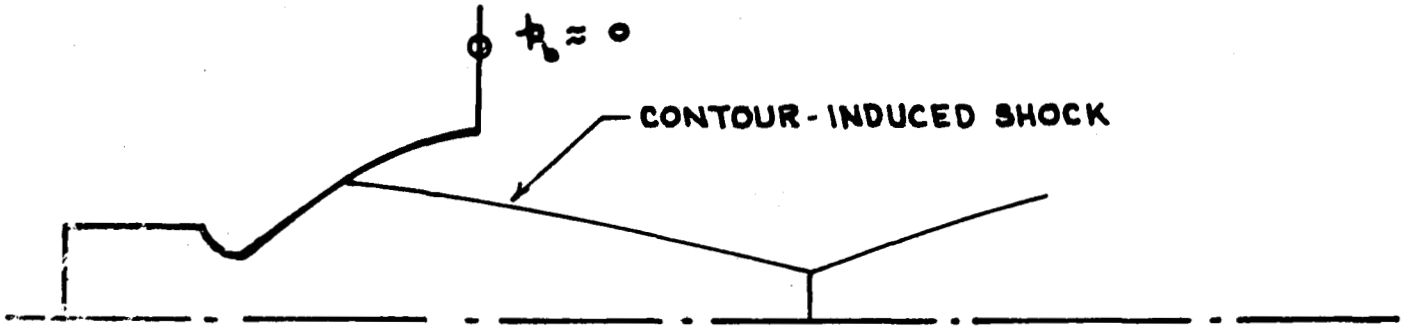

(a) CONTOUR ASCENT NOZZLE - NO DESCENT STAGE

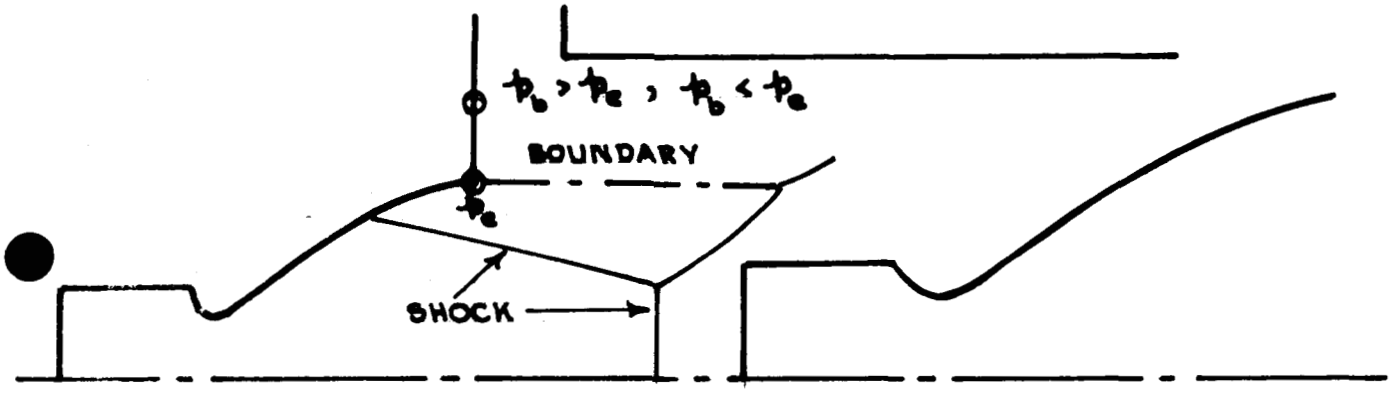

(b) CONTOUR ASCENT NOZZLE - DESCENT STAGE WITH 1240 IN^2 OF DOWNSTREAM VENT AREA

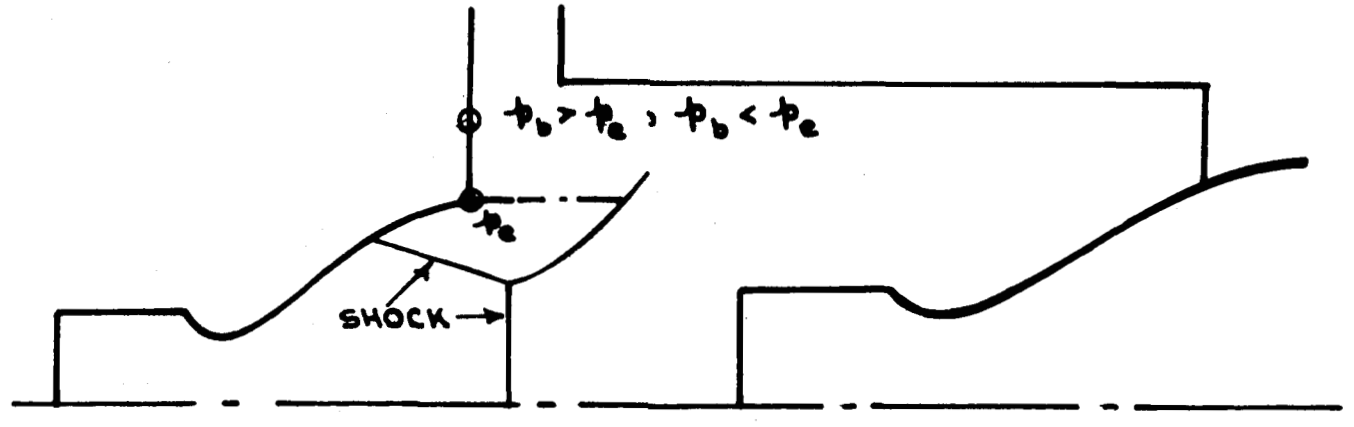

(c) CONTOUR ASCENT NOZZLE - DESCENT STAGE WITH SUFFICIENT SIDE VENTING TO PREVENT NOZZLE SEPERATION

FIGURE 1 (CONTINUED)

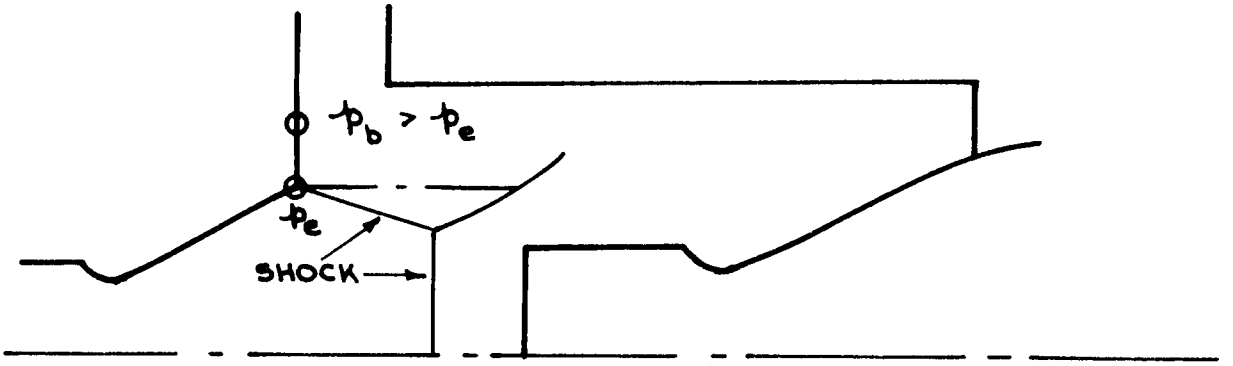

(d) CONICAL ASCENT NOZZLE - DESCENT STAGE WITH SIDE VENTING - NOZZLE OVEREXPANDED & FLOWING FULL

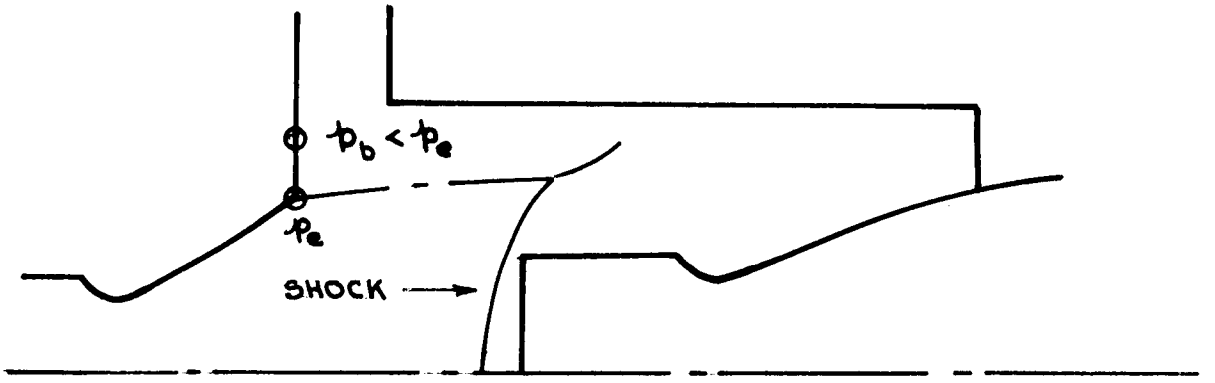

(e) CONICAL ASCENT NOZZLE - DESCENT STAGE WITH SIDE VENTING - NOZZLE UNDEREXPANDED

FIGURE - 1 (CONCLUDED)

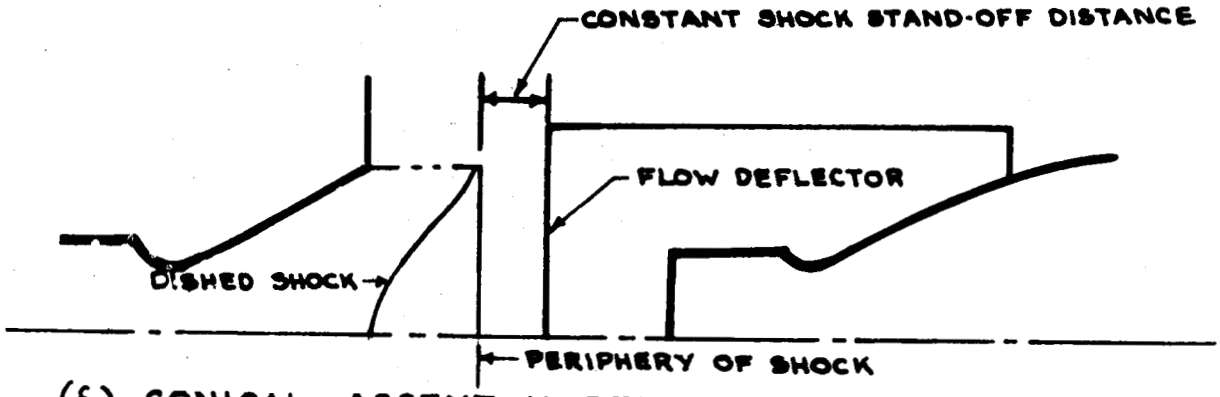

(f) CONICAL ASCENT NOZZLE - DESCENT STAGE WITH SIDE VENTING & FLAT PLATE FLOW DEFLECTOR

FIGURE - 2

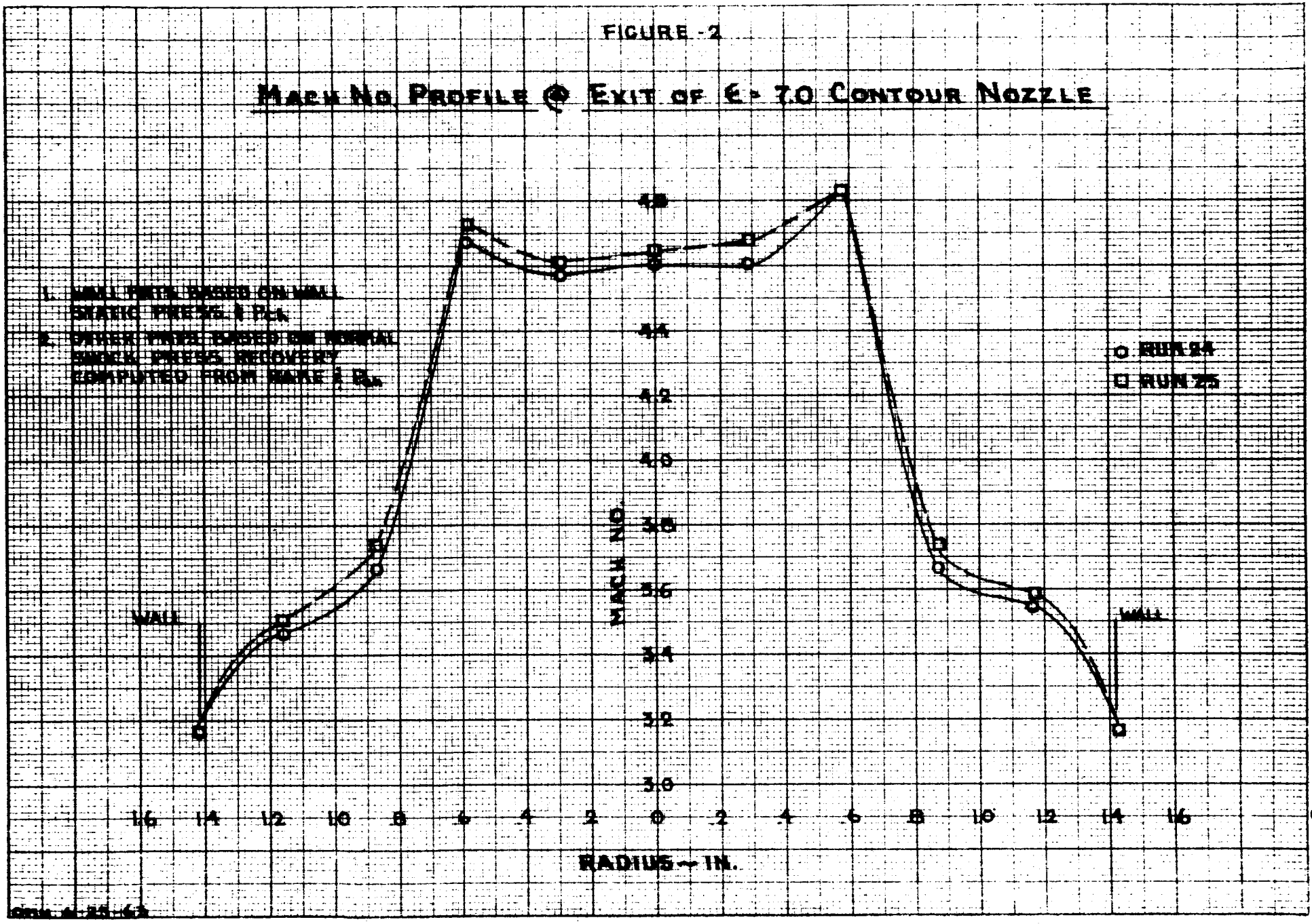

Contract No. NAS 9-1100
Primary Code No. 702

Report No. LED 510-3
Dated 23 July 1963

FIGURE - 5

ASCENT STAGE BASE PRESSURE TEST DATA

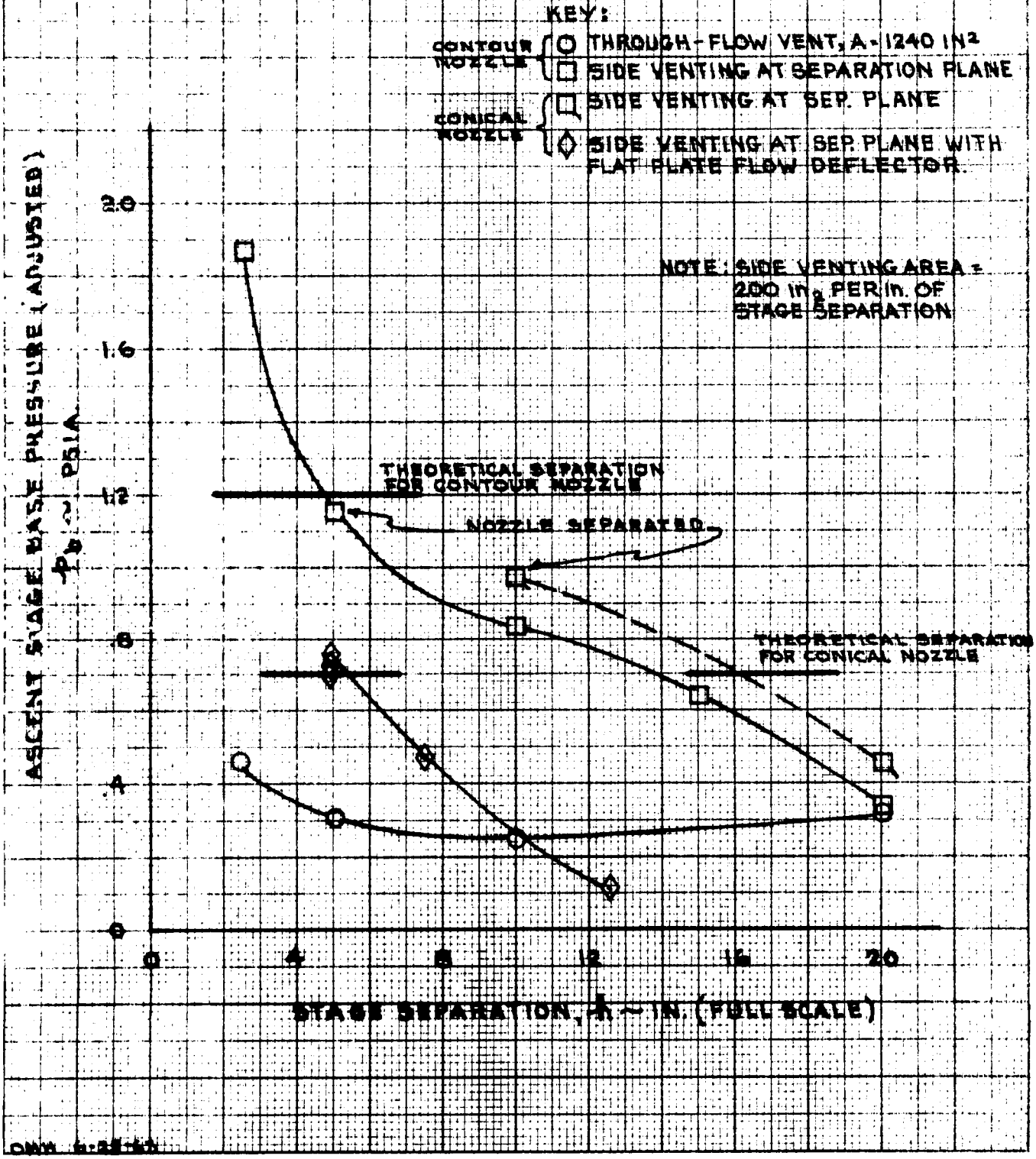

FIGURE - 4

ANALYTICAL MODEL OF A CONFIGURATION WITH SIDE PORTS LOCATED DOWNSTREAM OF DESCENT ENGINE FACE

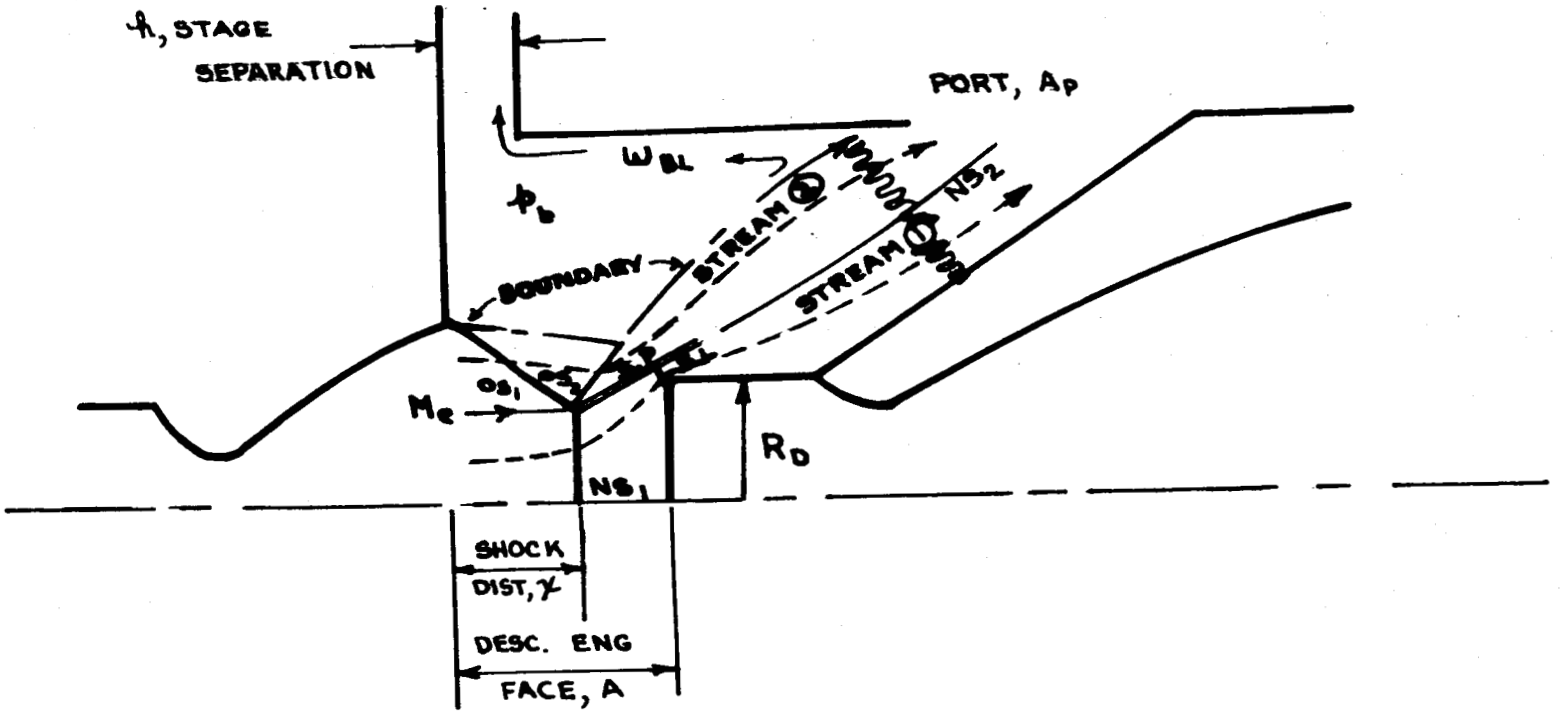

ASSUMPTIONS:

(1.) M_e = CONST.

(2.) NOZZLE IS OVEREXPANDED i.e, $p_b > p_e$

(3) TWO-DIMENSIONAL SHOCK SYSTEM (OS_1, OS_2, NS_1) FORMED AT NOZZLE LIP DUE TO OVEREXPANSION

(4) STREAMS 1 & 2 HAVE EQUAL STATIC PRESSURE & FLOW DIRECTION BEHIND NORMAL SHOCK (NS_1) YIELDING SLIP PLANE (SP)

(5) STREAM 1 REEXPANDS TO SONIC IN ANNULUS (S.L) NORMAL TO SP

(6) STREAMS 1 & 2 REEXPAND TO CAVITY PRESSURE p_b AND PASS THRU NORMAL SHOCK (NS_2) BEFORE LEAVING PORT.

(7) BLEED FLOW (W_{BL}) IS CHOKED IN ANNULUS BETWEEN STAGES, WITH TOTAL PRESSURE = p_b

Contract No. NAS 9-1100
Primary Code No. 702

Report No. LED 510-3
Dated 23 July 1963

FIGURE 5

PORT AREA REQUIRED

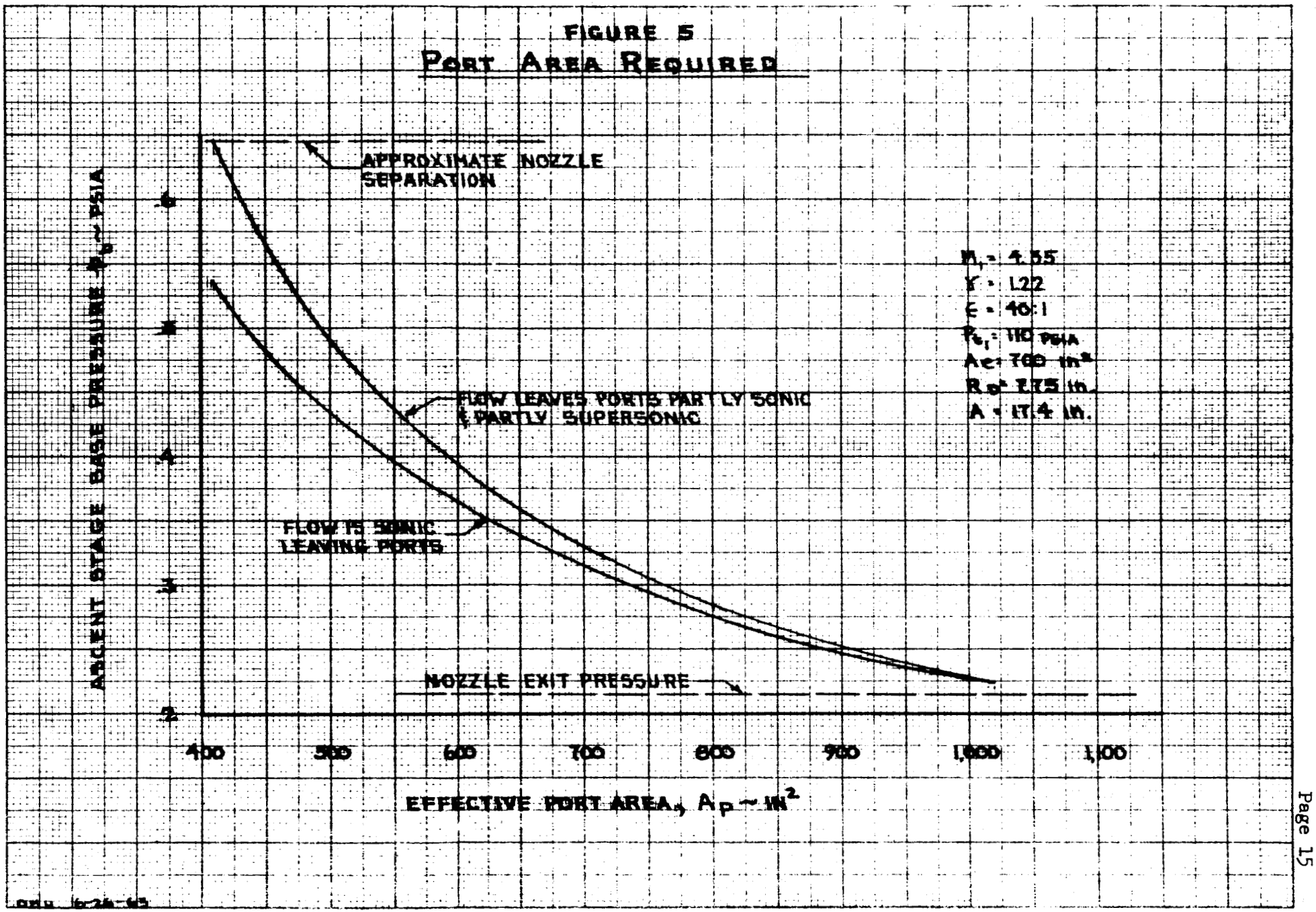

Contract No. NAS 9-1100
Primary Code No. 702

Report No. LED 510-3
Dated 23 July 1963

FIGURE 6

EFFECT OF DESCENT ENGINE LOCATION ON ASCENT STAGE BASE PRESSURE

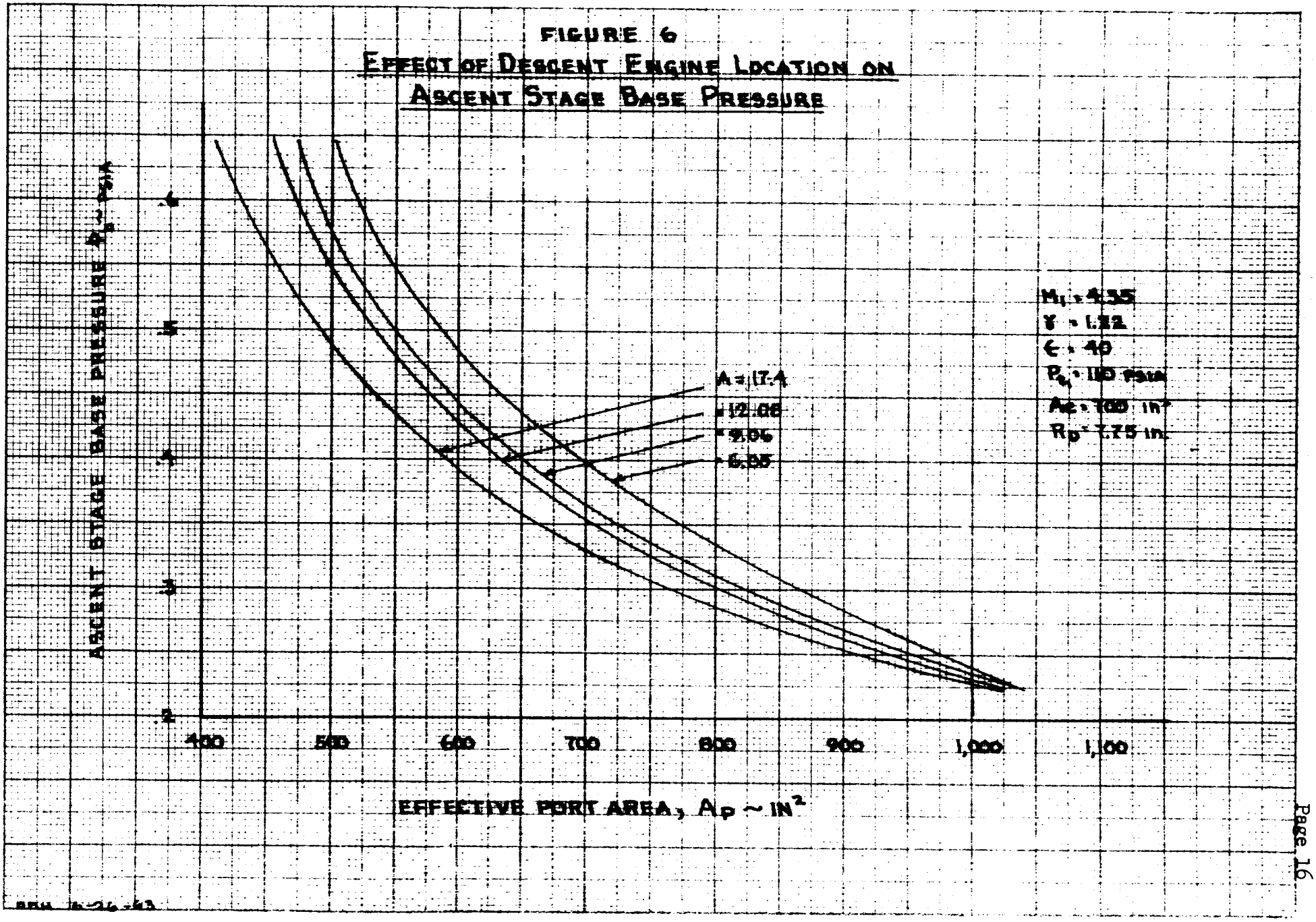

FIGURE 7

EFFECT OF BLOCKAGE ON ASCENT STAGE BASE PRESSURE

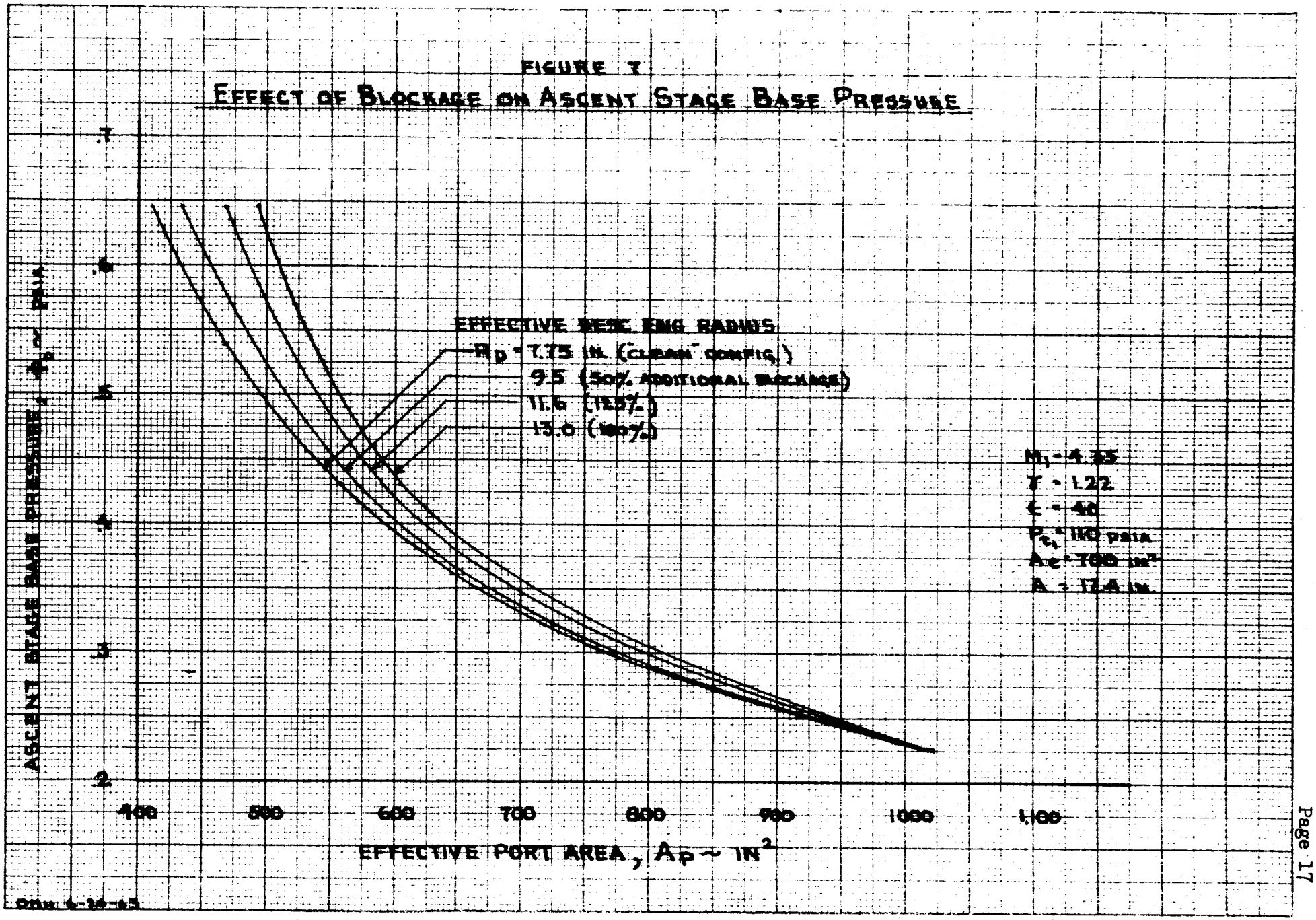

Contract No. NAS 9-1100
Primary Code No. 702

Report No. LED 510-3
Dated 23 July 1963

FIGURE 8

PRESSURE & MACH NO. SCALING REQUIRED (A) FOR A TEST FLUID WITH $\gamma = 1.3$

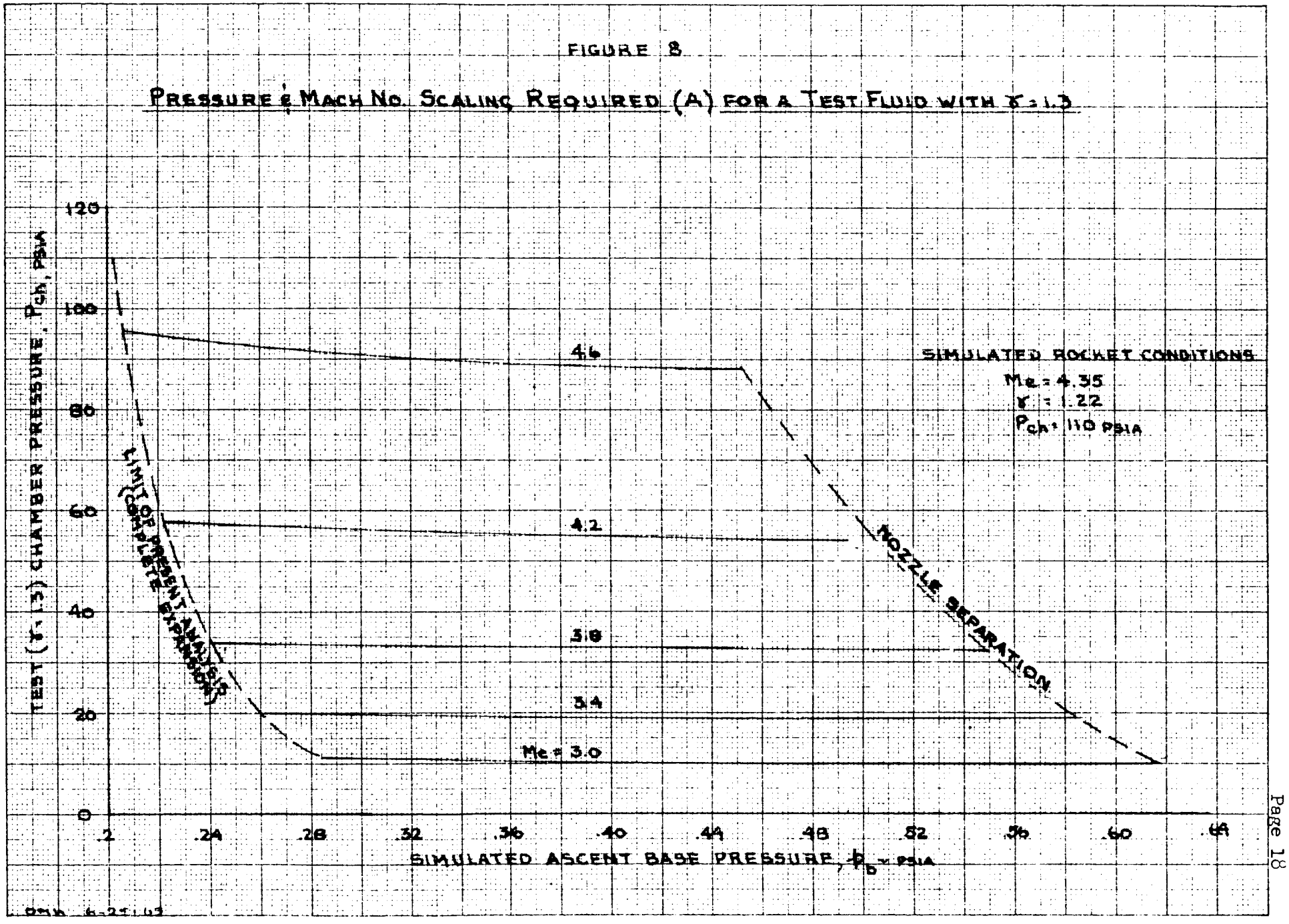

FIGURE 8

PRESSURE & MACH NO. SCALING REQUIRED (B) FOR A TEST FLUID WITH $\gamma = 1.4$

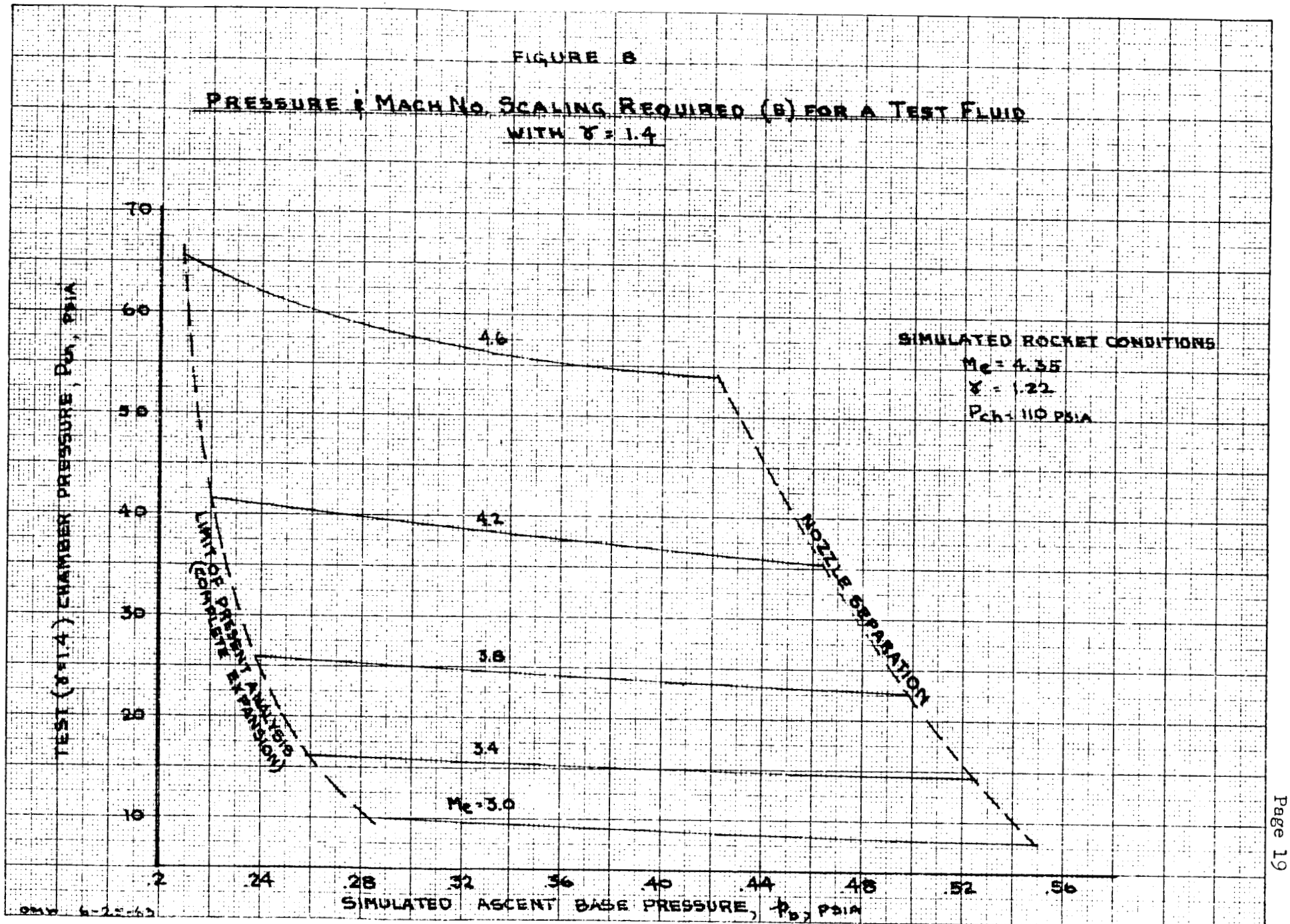

Contract No. NAS 9-1100
Primary Code No. 702

Report No. LED 510-3
Dated 23 July 1963

FIGURE 9

COMPARISON OF SCALING LAWS DERIVED FROM ANALYTICAL MODEL AND BASE FLOW TESTS. ($\gamma = 1.4$)

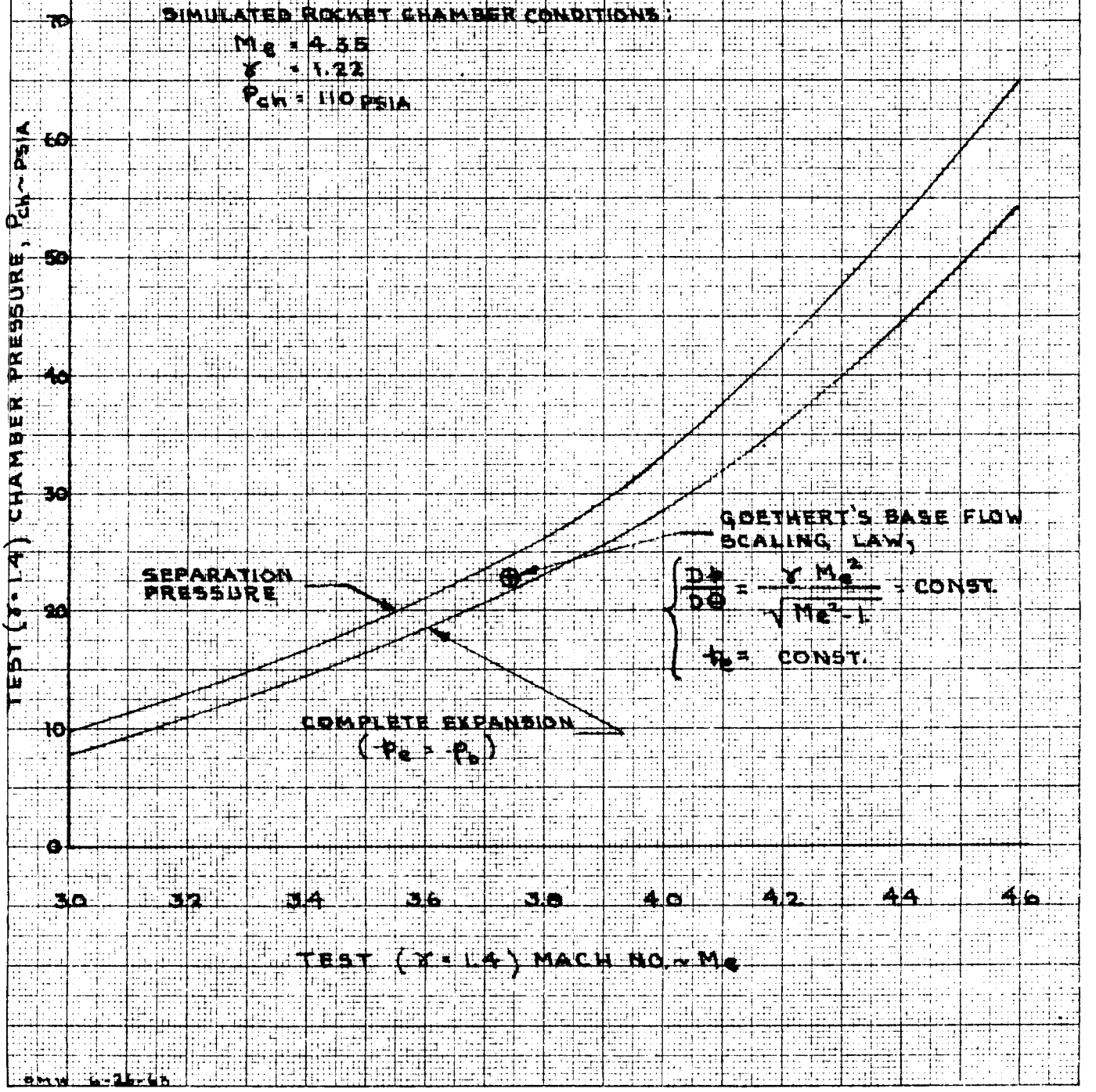

FIGURE - 10

ANALYSIS OF A CONFIGURATION WITH A FLOW DEFLECTOR AND SIDE VENTING BETWEEN THE STAGES

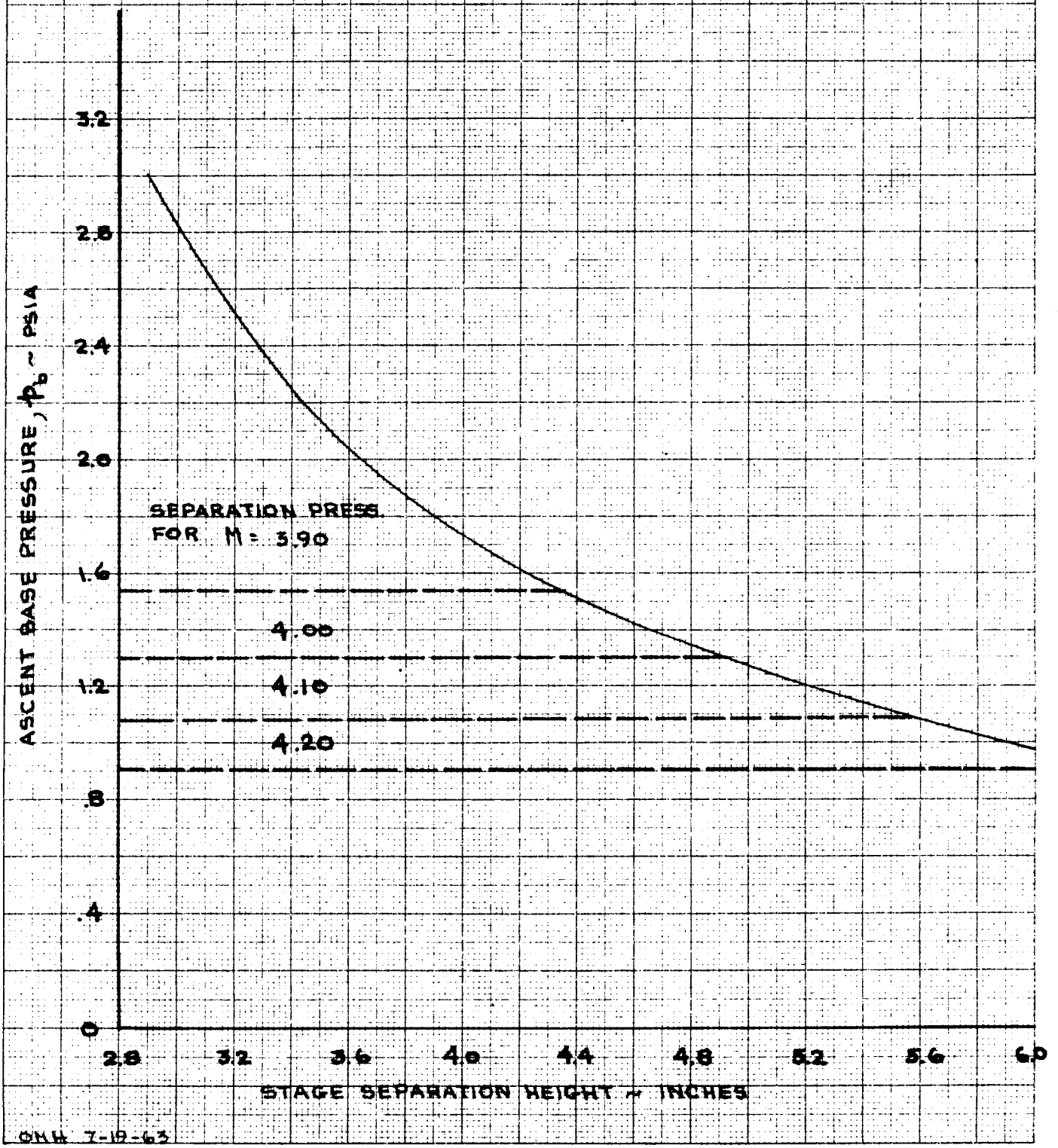

OMH 7-19-63

BIBLIOGRAPHY

1. Haslett, R. A., "Preliminary Fire-in-the-Hole Study", Grumman LED-510-1, April 3, 1963 - "Confidential"

2. Dunkerley, C. L., "Test Procedure for the LEM Fire-in-the-Hole Model Tests", Grumman LMO-510-36, July 24, 1963

3. Goethert, B. H., and Barnes L. T., "Some Studies of the Flow Pattern at the Base of Missiles with Rocket Exhaust Jets", AEDC TR-58-12 (Revised) June 1960.

4. Goethert, B. H., "Studies of the Flow Characteristics and Performance of Multi-Nozzle Rocket Exhausts", AEDC TR-59-16, October 1959 - "Confidential"

5. Korst, H. H., Page, R. H., and Childs, M. E., "A Theory for Base Pressures in Transonic and Supersonic Flow", University of Illinois, ME TN 392-2, March 1955